J. Opt. B: Quantum Semiclass. Opt. **1** (1999) 469–474. Printed in the UK PII: S1464-4266(99)01137-4

# Optimization and transfer of vacuum squeezing from an optical parametric oscillator

**P K Lam†, T C Ralph†, B C Buchler†, D E McClelland†, H-A Bachor† and J Gao‡**

† Department of Physics, Faculty of Science, The Australian National University, Canberra, ACT 0200, Australia
‡ Institute of Opto-Electronics, Shanxi University, Taiyuan, Shanxi, People's Republic of China

E-mail: Ping.Lam@anu.edu.au

Received 20 January 1999

**Abstract.** We report the observation of more than 7 dB of vacuum squeezing from a below-threshold optical parametric oscillator (OPO). We discuss design criteria and experimental considerations for its optimization and demonstrate that the vacuum squeezing can be electro-optically transferred to a bright beam using a feed-forward loop. This is compared with the bright intensity squeezed beam generated by running the OPO as a de-amplifier.

**Keywords:** Optical parametric oscillation, squeezed light, quantum noise, electro-optic control

## 1. Introduction

Squeezed states of light offer the potential of improving the performance of optical devices. They can, partially, eliminate the limiting effects of quantum noise [1]. Some of the earliest [2], and certainly some of the largest noise suppressions with squeezed light [3, 4] have been achieved by using a below-threshold optical parametric oscillator (OPO). These experiments generated the so-called '*squeezed vacuum*' states. These are beams of light with very low photon numbers (generated by the parametric process), which cannot be observed by direct photodetection. In contrast, '*bright squeezed*' states have sufficiently large intensity to allow direct photocurrent measurements. Based on this classification the sub-threshold OPO generates squeezed vacuum states while frequency doublers, Kerr media and laser diodes produce bright squeezed states. A third category is '*twin beam squeezing*' [5, 6], generated by an above threshold OPO, where the difference in the intensity of the two output beams has noise variance below the standard quantum limit.

Which type of squeezed light is desirable is dependent on the application. For example, improvements in sensitivities in spectroscopic measurement [7], velocimetry [8] and small signal communication require bright squeezed light. In interferometers [9, 10] and polarimeters [11], a squeezed vacuum state is usually required. Absorption experiments can be performed with twin beam squeezing [6]. In quantum non-demolition (QND) measurement and teleportation [12] there may be advantages for either bright or squeezed vacuum light, depending on the details of the proposed scheme. In general, it is desirable to generate squeezed light that allows independent control of the degree of squeezing, the intensity of the beam and possibly the quadrature angle of the squeezing.

In this paper, we report 7 dB of measured vacuum squeezing from an OPO output and discuss the technical limits to the observable squeezing of our system. In addition, we demonstrate and compare two different approaches for the generation of bright squeezed light. The first, more conventional, approach is by seeding the OPO and operating it as an optical parametric amplifier (OPA). Such a system produces bright phase squeezed light when the phase of the seed beam $\Phi_{\text{seed}}$ relative to the pump is adjusted for the OPA to act as an amplifier. In contrast, the output is intensity squeezed when $\Phi_{\text{seed}}$ is changed by $\pi/2$ and the system de-amplifies the input intensity [13].

An alternative method is to mix the squeezed vacuum output from the OPO on a beamsplitter with a coherent beam. This technique is wasteful in laser energy since a very asymmetric beamsplitter is required to preserve most of the squeezing. An improvement to this method is to use a feedforward control loop to electro-optically transfer the squeezing from one output of the beamsplitter to the other [14]. Similar schemes to this employing feedback loops have previously been proposed [15, 16]. In this way it is possible to recover most of the noise suppression, within the limits set by the photodetector efficiencies, without requiring an asymmetric beamsplitter. We discuss this technique in

1464-4266/99/040469+06$30.00  

detail and demonstrate squeezing transfer with our strongly squeezed vacuum beam.

## 2. Theoretical description of an OPO

We model the parametric process with the following simple approach. The Hamiltonian of the parametric down-conversion process can be written as [17]

$$\hat{H} = E\hat{a}^\dagger\hat{a}^\dagger - E\hat{a}\hat{a} \tag{1}$$

where $E$ is, in general, a complex constant that is dependent on the nonlinearity and the pump intensity of the OPO, which is assumed to be undepleted. $\hat{a}$ and $\hat{a}^\dagger$ are the annihilation and creation operators of the degenerate OPO output mode. The equations of motion of the OPO can then be written as

$$\dot{\hat{a}} = E\hat{a}^\dagger - \gamma\hat{a} + \sqrt{2\gamma_b}\hat{A}_b + \sqrt{2\gamma_l}\,\delta\hat{A}_l + \sqrt{2\gamma_c}\delta\hat{A}_c \tag{2}$$

$$\dot{\hat{a}}^\dagger = E^*\hat{a} - \gamma\hat{a}^\dagger + \sqrt{2\gamma_b}\hat{A}_b^\dagger + \sqrt{2\gamma_l}\delta\hat{A}_l^\dagger + \sqrt{2\gamma_c}\delta\hat{A}_c^\dagger \tag{3}$$

where $\gamma_b$, $\gamma_c$ and $\gamma_l$ are the decay rates due to the back and front reflectivities and the intra-cavity losses of the OPO; $\gamma = \gamma_b + \gamma_c + \gamma_l$ is the total cavity decay rate; $\hat{A}_b$ is the seed wave injected at the back face of the OPO and $\delta\hat{A}_c$ and $\delta\hat{A}_l$ are the vacuum fluctuations terms associated with the respective losses. The steady state solution for the expectation of $\hat{a}$, $\langle\hat{a}\rangle = \alpha$, can be found by setting the above derivatives to zero and ignoring quantum fluctuations,

$$\alpha = \frac{E}{\gamma}\alpha^* + \frac{\sqrt{2\gamma_b}}{\gamma}A_b \tag{4}$$

$$\alpha^* = \frac{E^*}{\gamma}\alpha + \frac{\sqrt{2\gamma_b}}{\gamma}A_b^*. \tag{5}$$

By assuming that $\langle A_b\rangle = A_b$ is a real number, we obtained a simple expression for the intra-cavity field,

$$\alpha = \frac{\sqrt{2\gamma_b}A_b(1 + E/\gamma)}{\gamma(1 - |E|^2/\gamma^2)}. \tag{6}$$

We note that in the absence of a pump amplitude, $A_b = 0$, the intra-cavity field has no coherent amplitude $\alpha = 0$. Using the input–output formalism, we can work out the extra-cavity transmitted and reflected fields, $A_{\text{trans}} = \sqrt{2\gamma_c}\,\alpha$ and $A_{\text{refl}} = \sqrt{2\gamma_b}\,\alpha - A_b$. The reflected and transmitted photon number expressions are

$$n_t = \left|\frac{2\sqrt{\gamma_b\gamma_c}(1 + E/\gamma)}{\gamma(1 - |E|^2/\gamma^2)}\right|^2 A_b^2 \tag{7}$$

$$n_r = \left|\frac{2\gamma_b(1 + E/\gamma)}{\gamma(1 - |E|^2/\gamma^2)} - 1\right|^2 A_b^2. \tag{8}$$

The quantum noise behaviour of the OPO can be obtained from equations (2) and (3). By taking the Fourier transform of the equations, we obtain expressions for the fluctuations $\delta\hat{X}_i^+ = \hat{a}_i + \hat{a}_i^\dagger$ of the amplitude quadrature and $\delta\hat{X}_i^- = \mathrm{i}(\hat{a}_i - \hat{a}_i^\dagger)$ of the phase quadrature of the field

$$\mathrm{i}\Omega\delta\tilde{X}^+ = (\mathrm{Re}[E] - \gamma)\delta\tilde{X}^+ + \mathrm{Im}[E]\delta\tilde{X}^- + \sqrt{2\gamma_b}\delta\tilde{X}_b^+ + \sqrt{2\gamma_l}\delta\tilde{X}_l^+ + \sqrt{2\gamma_c}\delta\tilde{X}_c^+ \tag{9}$$

$$\mathrm{i}\Omega\delta\tilde{X}^- = \mathrm{Im}[E]\delta\tilde{X}^+ + (\mathrm{Re}[E] + \gamma)\delta\tilde{X}^- + \sqrt{2\gamma_b}\delta\tilde{X}_b^- + \sqrt{2\gamma_l}\delta\tilde{X}_l^- + \sqrt{2\gamma_c}\delta\tilde{X}_c^- \tag{10}$$

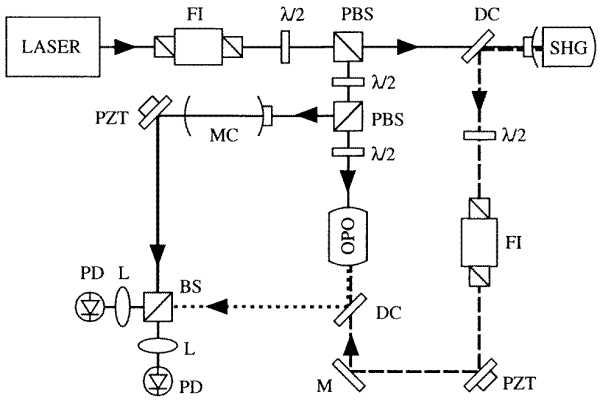


**Figure 1.** Schematic of the OPO experimental arrangement. Solid, dashed and dotted lines are the 1064 nm laser, second harmonic and vacuum squeezed light beams, respectively. M: mirror, FI: Faraday isolator, PZT: piezo-electric actuator, DC: dichroic beamsplitter, L: lens, PD: photodetector, (P)BS: (polarizing) beamsplitter, $\lambda/2$: half-wave plate, SHG: second-harmonic generator and MC: mode cleaner cavity.

where all $\delta\tilde{X}_i = \delta\tilde{X}_i(\Omega)$ are now operators as a function of the detection angular frequency, and $\mathrm{Re}[E]$ and $\mathrm{Im}[E]$ denote the real and imaginary part of the complex number $E$. The internal and the external fields are again linked by the input–output formalism, $\delta\tilde{X}_1^+(\Omega) = \sqrt{2\gamma_c}\delta\tilde{X}^+(\Omega) - \delta\tilde{X}_c^+(\Omega)$, where the subscript 1 is used to denote the measurable output mode of the OPO. The noise spectrum $V^+(\Omega)$ of the output is then obtained using

$$V^+(\Omega) = \langle\delta\tilde{X}_1^{+*}(\Omega)\delta\tilde{X}_1^+(\Omega)\rangle. \tag{11}$$

This spectrum contains the information about the amplitude quadrature of the OPO which is measured in our experiment. The expression for the phase quadrature variance of the OPO $V^-$ can be similarly obtained.

## 3. Experimental set-up

The experimental set-up of the OPO is as shown in figure 1. A 700 mW diode pumped Nd:YAG non-planar ring laser (LZH 700) is used to pump a second-harmonic generator (SHG). The SHG consists of a hemilithic MgO:$LiNbO_3$ crystal which is 7.5 mm in length with one surface polished to a radius of 10 mm and coated as a high reflector ($R > 99.96\%$) at 1064 and 532 nm. The other surface is polished flat and anti-reflection coated ($R < 0.1\%$) at both wavelengths. The cavity output coupler is a separate mirror placed 21.3 mm from this end of the hemilith. The cavity has a waist of 27 $\mu$m in diameter for 1064 nm located at the centre of the hemilithic crystal. The output coupler of the SHG is 96% reflecting at 1064 nm and 10% reflective at 532 nm. The cavity is temperature stabilized to $\pm 2$ mK. A hemilithic design makes cavity locking easier compared with a monolithic cavity since the reflection locking error-signal can be used to actuate a piezo on the cavity output coupler. When optimized, this system has a maximum conversion efficiency of 60% and generates 300 mW of single-mode second harmonic output.

The green SHG output is used to pump the OPO. This is a monolithic MgO:$LiNbO_3$ crystal, 7.5 mm in length, with an

output coupler 4% reflective to 532 nm and 95.6% reflective to 1064 nm. The other end is a high reflector with 99.96% for both wavelengths. The intra-cavity losses of the material is low (about 0.1% $cm^{-1}$ at 1064 nm and about 4% $cm^{-1}$ at 532 nm). The cavity parameters give a finesse of $F = 136$, free spectral range FSR = 9 GHz and cavity linewidth of 67 MHz. The surfaces have radii of curvature of 10 mm which produce a waist of 27 $\mu$m for the 1064 nm mode. The crystal is gold coated on the surfaces orthogonal to the crystal optical axis for the application of an electric field. This can be used for tuning of the refractive index, and therefore the resonance condition, of the cavity. The OPO crystal is only 2.5 mm thick which allows for a large electric field gradient and therefore a larger tuning range. The temperature of the OPO is also controlled to $\pm 2$ mK.

The third major component of the experiment is the mode cleaning cavity. The output of the mode cleaner is a pure $TEM_{00}$ mode which can be matched on a beamsplitter to make a homodyne measurement of the squeezed beam generated by the OPO. Our mode cleaner has a finesse of 5000 and a linewidth of 176 kHz. At frequencies well above the cavity linewidth, the intensity noise of the transmitted beam is at the standard quantum limit which is advantageous for homodyning with a squeezed field. A servo system is used to lock the laser frequency to the mode cleaner. By varying the d.c. voltage applied to a piezo actuator on the mode cleaner, the cavity length is altered. This changes the laser frequency and therefore provides sensitive control of the phase matching condition of the pump beam to the OPO. The squeezing generated by the OPO can therefore be optimized by tuning the mode cleaner length. This system is stable for about several minutes before the laser frequency requires re-tuning. For stable squeezing the laser frequency and the OPO must be locked by an additional servo loop, a feat which remains a goal for future research.

## 4. Limits to vacuum squeezing

In most publications squeezing is analysed as a function of pump power. This is because the pump level normally determines the amount of squeezing. In the case of a below threshold OPO, 100% squeezing is predicted at the threshold in an ideal set-up. However, while the OPO is experimentally running below threshold, this is not the easiest quantity to measure since many other experimental conditions may vary. For example, the phase matching of the OPO crystal may have drifted due to the variation of pump light, thus causing a change in the OPO threshold.

A more systematic way of analysing the situation is a plot of the anti-squeezing quadrature versus the squeezing quadrature. As reported by Wu *et al* [2] the output of a below threshold OPO can be inferred to be a minimum uncertainty state. This piece of information can then be use to determine the efficiencies of the system and the amount of parametric action occurring at the below threshold condition.

The quantum noise analysis of the OPO gives us the following analytic expressions of the squeezing and anti-squeezing quadrature noise variance,

$$V^{+}(\Omega) = 1 - \eta_{\rm esc}\eta_{\rm det}\eta_{\rm hom}\frac{4\sqrt{P/P_{\rm thr}}}{(\Omega/\gamma)^2 + \left(1+\sqrt{P/P_{\rm thr}}\right)^2} \quad (12)$$

$$V^{-}(\Omega) = 1 + \eta_{\rm esc}\eta_{\rm det}\eta_{\rm hom}\frac{4\sqrt{P/P_{\rm thr}}}{(\Omega/\gamma)^2 + \left(1-\sqrt{P/P_{\rm thr}}\right)^2}. \quad (13)$$

Where $\eta_{\rm esc}, \eta_{\rm det}, \eta_{\rm hom}$ are the escape, detection and homodyne efficiencies of the OPO system; $P$ and $P_{\rm thr}$ are the pump and threshold powers, respectively. We now examine each limiting factor in detail.

*Escape efficiency*. The escape efficiency of the OPO is the ratio of output coupling decay rate to the total cavity decay rate given by $\eta_{\rm esc} = \gamma_c/\gamma$. From the parameter values, we obtained $\eta_{\rm esc} = 0.96 \pm 0.01$. Obviously, the escape efficiency can be increased by reducing the reflectivity of the OPO front face. However, this is at the expense of a much larger OPO threshold. Thus a further increase in the escape efficiency is only feasible with a more efficient SHG source or more powerful pump laser.

*Detection efficiency*. A pair of ETX-500 InGaAs photodiodes from Epitaxx were used in this experiment. The quantum efficiency of these photodetectors is $\eta_{\rm det} = 0.94 \pm 0.02$ and the detector is capable of detecting 10 mW of optical power without saturation with appropriate RF amplification circuit [18]. In our experiment, the squeezed vacuum is measured in a homodyne set-up with a 6 mW optical local oscillator. More than 10 dB of quantum noise floor clearance from the dark noise of the photodetector was present and hence the squeezed vacuum measurement does not require any electronic noise floor correction.

*Homodyne efficiency*. With the use of the spatial mode cleaner, the homodyne efficiency of our OPO system is $\eta_{\rm hom} = 0.97 \pm 0.02$.

*Cavity linewidth*. Another advantage of lowering the reflectivity of the OPO front face, or increasing the escape efficiency, is the broadening of the OPO cavity linewidth. Since squeezing is only observable within the cavity linewidth due to the input–output coupling, a larger linewidth is desirable. The linewidth of our OPO cavity is 67 MHz. At the detection frequency of this experiment (3 MHz), linewidth considerations are unimportant.

*Threshold power*. Investigations of the regenerative gain of the OPO have revealed that the available second harmonic power of the system is sufficient to get within 2% of the threshold power. From equations (12) and (13), we note that the amount of vacuum squeezing has only a square-root dependence on the pump power of the OPO. Hence, this factor is not crucial. In fact, the best vacuum squeezing results from OPO were obtained at a level significantly lower than the OPO threshold due to the phase stability of the system.

*Phase jitter*. Phase angle resolution becomes more and more acute with larger squeezing. The vibration of the reflecting surfaces causes jitter in the relative phase of the local oscillator and the squeezed beam. If these vibrations are faster than the time required for the spectrum analyser to gather a single pixel of information, then that point will not be a pure measurement of the noise at quadrature phase angle $\theta$. Instead it will be a measurement of the noise integrated over some range of angles $\theta \pm \delta\theta$. If this happens, then some of the noise from the anti-squeezed quadrature is coupled into what was intended to be a measurement of the squeezed quadrature. This will reduce the amount of squeezing which can be observed. Figure 2 shows a theoretical prediction

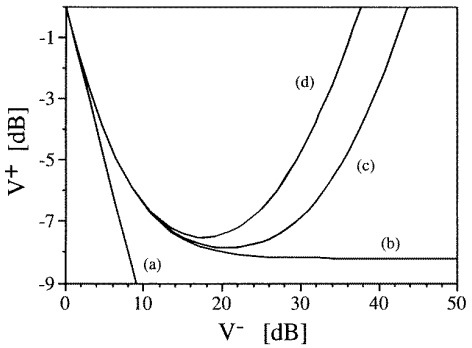


**Figure 2.** Limits imposed on the observable squeezing. (*a*) Theoretical value of an ideal system with minimum uncertainty state output; (*b*) calculated squeezing after experimental efficiencies are considered; (*c*) addition of 3° of phase jitter and; (*d*) 6° phase jitter. In the presence of phase jitter, there is an optimum pump level below threshold which produces the largest observable squeezing.

of the observable squeezing of $V^+$ as a function of the anti-squeezing quadrature $V^-$. With a perfectly efficient system, trace (*a*) shows the reduction of noise in the squeezed quadrature $V^+$ and the corresponding increase of noise in the anti-squeezed quadrature $V^-$ predicted by equations (12) and (13). When experimental efficiencies are included, trace (*b*) shows that as the OPO approaches threshold, the observable squeezing is limited by the experimental efficiencies to a maximum of 8.5 dB close to threshold, while the anti-squeezing noise still increases. The addition of phase jitter, shown in traces (*c*) and (*d*), means that as the OPO approaches threshold, increasingly large amounts of noise are coupled into the measurement of $V^+$ and the amount of squeezing observed actually decreases.

## 5. Classical regenerative gain

Because of the large escape efficiency of our OPO, the available second harmonic power is insufficient to pump the OPO above threshold. The initial investigation into the characteristics of the OPO is therefore performed by running the OPO as an amplifier with an input seed wave. Figure 3 shows the calculated results of the OPA gain using equation (7), assuming that the pump power is not significantly depleted. We note that close to the threshold, the OPA gain obtained from the transmitted beam can be very large ($G > 10\,000$ or 50 dB). This is due in part to the parametric amplification and in part to the improvement of the cavity impedance matching.

The impedance matching condition of a cavity is given by [19]

$$\Delta M = \sqrt{R_c} - \sqrt{R_b}(1 - L) = 0 \qquad (14)$$

where $R_c$ and $R_b$ are the reflectivities of the back and front surfaces, and $L$ is the total intra-cavity loss. We note that without any incident pump field, the coupling and transmission of the seed wave from the back of the OPO is very small, due to the poor impedance matching (large $\Delta M$ due to $R_c > R_b(1 - L)$) of the OPO cavity. When the OPO is pumped by an incident wave, parametric gain is experienced by the sub-harmonic mode. This corresponds

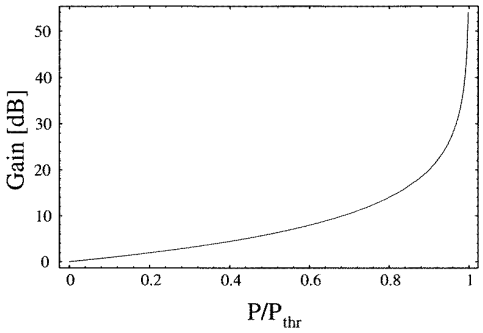


**Figure 3.** Classical gain of the OPO, assuming undepleted pump, as a function of pump power. The gain is calculated by considering the ratio of transmitted powers with OPO pump power on and off, $P_{\rm inc} = P$ and $P_{\rm inc} = 0$

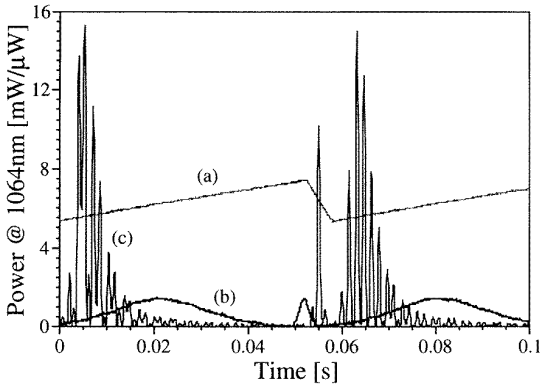


**Figure 4.** Measured maximum classical gain of the OPO. The OPO is electro-optically modulated by application of a ramp voltage with a period of 55 ms as shown in trace (*a*). Trace (*b*) shows the small input signal beam injected at the back face of the OPO, the peak power of the input beam corresponds to 1.5 $\mu$W of optical power. With the pump field of the OPO turned to the maximum of 300 mW, trace (*c*) shows the transmitted output. We note that the presence of the pump field slightly shifted the resonance of the OPO due to the thermal effect caused by pump absorption. The pump field is modulated at a much shorter period of 3 ms. Parametric amplification or de-amplification is observed when the pump field is in-phase or in-quadrature with the signal field. The maximum classical gain achieved is ≈10 000 (15 mW).

to having a negative loss $L < 0$, thus making the cavity better impedance matched. Thus, more of the seed wave is coupled into the OPO, resulting in even more gain. Figure 4 shows a regenerative OPO gain of $\approx$ 10 000 when all of the available pump power from the SHG is incident on the OPO. We note that this corresponds to within 2% of the theoretically calculated threshold. However, in spite of attempts to increase the second harmonic output, above-threshold oscillation of the OPO was not observed.

## 6. Squeezing results

Figure 5 shows the end results of our optimization of all experimental parameters. At a pump power of around $60 \pm 10\%$, we observed our best vacuum squeezing results of more than $7.0 \pm 0.2$ dB.

Figure 6 shows the bright intensity squeezing observed with a small seed wave injected at the back face of the

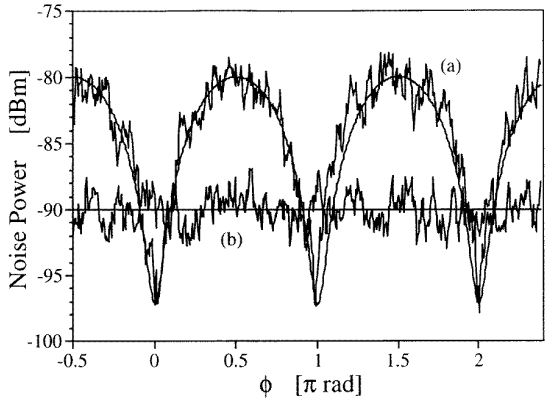


**Figure 5.** Noise variance of the squeezed vacuum. Trace (*a*) shows experimental results of the noise variance measurement of the squeezed vacuum state. The scan measurement of the quadrature phase shows a variation of noise variance from 10 dB above the standard quantum limit to more than 7 dB of quadrature squeezing. The smooth line is fitted values of a 7.1 dB squeezed vacuum assuming the given experimental efficiencies. The standard quantum noise level is at −90 dB m as shown by trace (*b*). ResBW = 50 kHz and VBW = 1 kHz.

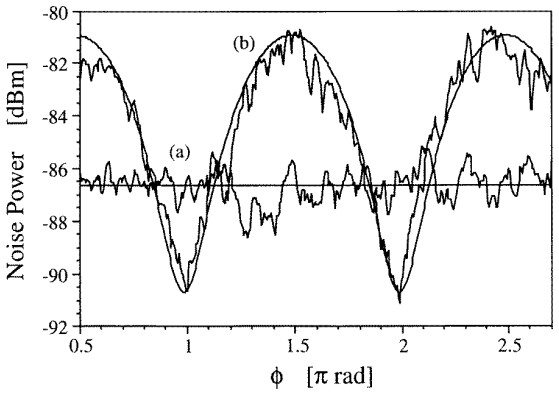


**Figure 6.** Noise variance of the output of the OPA. Trace (*a*) shows the noise variance scan of the OPA output. The noise variance varies from 5.5 dB above the standard quantum limit to close to 4 dB of quadrature squeezing. (*b*) shows the quantum noise limit at −86.6 dB m. The measurements obtained with the OPA are not as reliable as the OPO vacuum squeezing due to problems with the locking system.

OPO. The relative phase of the pump with the injected seed were locked by observing the minimum d.c. level of the sum photocurrents of the homodyne detectors. This corresponds to the de-amplification condition of the OPA which is predicted to produce amplitude quadrature (intensity) squeezing. More than 4 dB of intensity squeezing is observed. However, the intensity squeezing obtained from the parametric de-amplification process provides a squeezed beam of relatively low intensity. When higher input seed powers are used, the intensity noise of the input beam becomes dominant. Unless the seed is quantum noise limited, squeezing obtained from the parametric process will be buried by the residual intensity noise of the seed wave.

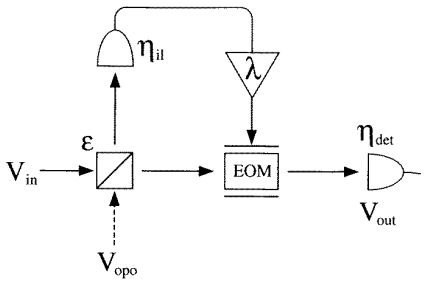


**Figure 7.** Electro-optic feedforward loop for the transfer of vacuum squeezing. $\eta_{\rm il}$: in-loop detector efficiency; $\eta_{\rm det}$: total detection efficiency of the transmitted beam, inclusive of transmission loss of the modulator.

## 7. Transfer of squeezing

Feedforward has been used previously [14] as a noiseless amplifier. Here we show an alternative use which is to transfer squeezing. When a squeezed vacuum beam is mixed on a beamsplitter to make bright squeezing, some of the squeezing is lost through the beamsplitter. Feedforward is implemented by detecting the lost squeezing and using that photocurrent to drive a modulator in the remaining beam as shown in figure 7. In our set-up feedforward is easily incorporated by rejigging the homodyne detector. One of the photodiodes in the homodyne system is used to drive an amplitude modulator in the remaining arm. The equation describing output variance of the photocurrent due to the beam with feedforward is given by [14]

$$V^+_{\rm out} = \eta_{\rm det}\left|\sqrt{\varepsilon}+\lambda\sqrt{\eta_{\rm il}(1-\varepsilon)}\right|^2 V^+_{\rm in} + \eta_{\rm det}\left|\sqrt{1-\varepsilon}-\lambda\sqrt{\eta_{\rm il}\varepsilon}\right|^2 V^+_{\rm opo} + \eta_{\rm det}(1-\eta_{\rm il})|\lambda|^2 + 1 - \eta_{\rm det}, \quad (15)$$

where $V^+_{\rm in}$ and $V^+_{\rm opo}$ are the intensity variance of the local oscillator and OPO respectively. $\eta_{\rm il}$ and $\eta_{\rm det}$ are the in-loop detection efficiency and the efficiency of final detection including any losses introduced by the modulator. $\lambda$ is the electronic gain of the feedforward loop. Assuming that the local oscillator is quantum noise limited, we can let $V^+_{\rm in} = 1$. The beamsplitter transmittance $\varepsilon$ is set to $\frac{1}{2}$ in our experiment.

In equation (15) we can see that the noise due to the local oscillator (first term) may be eliminated through careful choice of negative gain, ie. negative $\lambda$. Negative gain will also have the effect of amplifying the noise introduced by the OPO (second term). However, provided this variance is squeezed, the reduction of the local oscillator noise will outweigh the amplification of the OPO noise. In fact the optimum gain is given by

$$\lambda = -\frac{\sqrt{\eta_{\rm il}\varepsilon(1-\varepsilon)}(1-V^+_{\rm opo})}{1-\eta_{\rm il}\varepsilon(1-V^+_{\rm opo})} \quad (16)$$

and at this point the maximum amount of squeezing is recovered on the output beam of the feedforward loop. The results of this method are shown in figure 8. The bright squeezing is 4 dB below the QNL which is significantly better than the 2 dB achieved with the 50/50 beamsplitter and no feedforward.

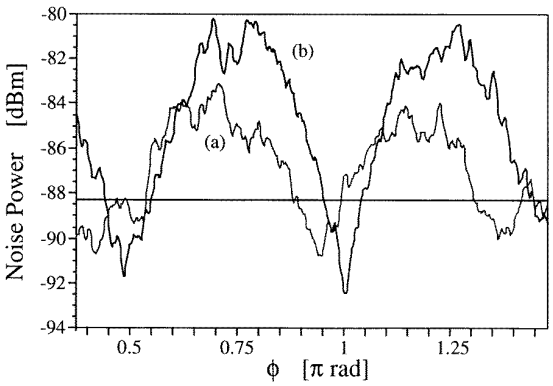


**Figure 8.** Noise variance of the output of the feedforward loop. Trace (*a*) shows the noise variance scan without feedforward. Trace (*b*) shows the effect with the optimum amount of negative feedforward. Close to 2 dB of squeezing is retrieved.

## 8. Conclusion

We report 7 dB of vacuum squeezing and believe that this is limited by the phase stability of our system as our predicted value for the best observable squeezing is at around 8.5 dB. We have shown that bright intensity squeezed light can be obtained by operating the OPO as an intensity de-amplifier. The best result obtained was 4 dB of intensity squeezing. Alternatively, bright intensity squeezed light can also be produced using a feedforward loop. The best result obtained was also 4 dB of squeezing.

## Acknowledgments

We acknowledge contributions through discussions with A G White, and M B Gray. We also thank A G White for his active participation during the design stage of the OPO. This research was supported by the Australian Research Council.

## References

[1] Kimble H J 1992 *Phys. Rep.* **219** 227
[2] Wu L-A, Xiao M and Kimble H J 1987 *J. Opt. Soc. Am.* B **4** 1465
[3] Ou Z Y, Pereira S F, Kimble H J and Peng K C 1992 *Phys. Rev. Lett.* **68** 3663
[4] Breitenbach G, Müller T, Pereira S F, Poizat J-Ph, Schiller S and Mlynek J 1995 *J. Opt. Soc. Am.* B **12** 2304
[5] Heidmann A, Horowicz R J, Reynaud S, Giacobino E, Fabre C and Camy G 1987 *Phys. Rev. Lett.* **59** 2557
[6] Gao J, Cui, F Xue C, Xie C and Peng K 1998 *Opt. Lett.* **23** 870
[7] Polzik E S, Carri J and Kimble H J 1992 *Appl. Phys.* B **55** 279
[8] Li Y-Q, Lynam P, Xiao M and Edwards P J 1997 *Phys. Rev. Lett.* **78** 3105
[9] Xiao M, Wu L A and Kimble H J 1987 *Phys. Rev. Lett.* **59** 278
[10] Gea-Banacloche J and Leuchs G 1987 *J. Opt. Soc. Am.* B **4** 1667
[11] Grangier P, Slusher R E, Yurke B and La Porta A 1987 *Phys. Rev. Lett.* **59** 2153
[12] Furusawa A, Serensen J L, Braunstein S L, Fuchs C A, Kimble H J and Polzik E S 1998 *Science* **282** 706
[13] Schneider K, Lang M, Mlynek J and Schiller S 1998 *Opt. Express* **2** 59
[14] Lam P K, Ralph T C, Huntington E H and Bachor H-A 1997 *Phys. Rev. Lett.* **79** 1471
[15] Caves C M 1987 *Opt. Lett.* **12** 971
[16] Buchler B C, Huntington E H, Harb C C and Ralph T C 1998 *Phys. Rev.* A **57** 1286
[17] Walls D F and Milburn G J 1994 *Quantum Optics* 1st edn (Berlin: Springer)
[18] Gray M B, Shaddock D A, Harb C C and Bachor H-A 1998 *Rev. Sci. Instrum.* **69** 3755
[19] Siegman A E 1986 *Lasers* 1st edn (CA: University Science Books)